

Comparison of PLS and kinetic models for a second-order reaction as monitored using ultraviolet visible and mid-infrared spectroscopy

Antonio R. de Carvalho, Miguel del Nogal Sánchez, Jirut Wattoo, Richard G. Brereton*

School of Chemistry, University of Bristol, Cantock's Close, Bristol BS8 1TS, UK

Received 17 December 2004; received in revised form 26 May 2005; accepted 15 July 2005

Available online 8 September 2005

Abstract

A second-order reaction between benzophenone and phenylhydrazine to give benzophenone phenylhydrazone was followed using UV/vis and mid-infrared spectroscopic probes. Established kinetic (hard) and partial least squares (soft) modelling chemometrics methods were applied to both datasets in order to compare the information acquired with each probe. To this purpose, an experimental design with 25 samples and a test set with 5 samples were used to build a partial least squares calibration model to predict the concentration profiles of the compounds present in the reaction vessel. In addition, multivariate kinetic modelling was also performed on the spectroscopic data. Using a guess of the rate constant, concentration profiles were estimated. The profiles are then used to calculate the estimated spectroscopic profile, which is compared to the data acquired experimentally. The residual is minimised and the rate constant estimated; this procedure is iterated until convergence. A total of four profiles were obtained for each compound, corresponding to two sets of probes and two sets of models. The results were compared and discussed. It is shown that several different spectroscopic techniques can be used in reaction monitoring, with increasing benefits in terms of information and interpretation of the results. The profiles obtained agreed well which was also demonstrated when comparing the different rate constants obtained.

© 2005 Elsevier B.V. All rights reserved.

Keywords: Online reaction monitoring; Ultraviolet visible spectroscopy; Mid-infrared spectroscopy; Partial least squares; Kinetic modelling

1. Introduction

Reaction monitoring using probes that can obtain spectroscopic data on-line as the reaction progresses has an important role to play especially in process chemistry. Over the past decade there has been a major expansion in NIR (near infrared) methods for reaction monitoring [1,2]. Traditionally, partial least squares (PLS) and related multivariate methods have been employed to determine the concentration of individual components from this on-line spectroscopic data, first developing a calibration model and then applying it to the mixture data, in order to estimate change in concentrations of the reactants from the spectroscopic data [3], especially to PLS in reaction monitoring and NIR [4].

However, over the last few years, a new generation of probes in the mid-infrared (MIR), ultraviolet visible (UV/vis) and Raman regions has been developed which promises to revolutionise reaction monitoring [5,6]. Coupled to this are new capabilities in analysis of the spectroscopic data using multivariate kinetic models [7] which has been an especially important growth point. The advantage of kinetic models is that they can incorporate extra information about the reaction that is often known in advance, for example the order of the reaction, and also that they do not require calibration standards. This has the advantage that there is no requirement for calibration using pure compounds: it is sometimes hard to perform calibration especially if the conditions under which a reaction is performed are unstable. Mixing the calibration standards under reaction conditions will lead to mixtures that do not have a long shelf life, for obvious reasons. Because spectra change with pH or temperature or most factors that catalyze a reaction [8], it is not always easy to develop a PLS

* Corresponding author. Tel.: +44 1179287658; fax: +44 1179251295.
E-mail address: r.g.brereton@bris.ac.uk (R.G. Brereton).

model under reaction conditions. Kinetics models, in contrast, depend on having a good knowledge of the reaction mechanism, often requiring one step reactions without significant intermediates or side products, and if the reaction is more than first order, it is necessary to know the concentration of starting materials. We can show that if some of this information is not accurately known this can result in poor predictions using kinetics methods [9].

We have previously studied the second-order reaction of benzophenone and phenylhydrazine [10,11] but using only kinetics models and a UV/vis probe. In analytical chemistry, it is often important to validate methods using independent approaches. One advance is to be able to monitor a reaction simultaneously using more than one probe, in this paper we report a reaction monitored using both a MIR and a UV/vis probe. Both have their advantages and disadvantages. MIR is a useful approach because compounds often show fairly characteristic spectral peaks that can be identified, but the MIR probe has a lower signal to noise ratio and individual spectra need to be recorded over a longer time period to obtain adequate intensity. Comparing results from both instruments is an important confirmation that our predictions are correct.

PLS models have been used for reaction monitoring [12–17], in some cases to obtain rate constants, but in many cases primarily to obtain reaction profiles, without kinetic information. The problem with PLS models in the context of this paper, is that the reaction is catalyzed by using acid, which also has a significant influence on spectral characteristics. Therefore, PLS calibration sets need to be recorded immediately after the acid is added. For the MIR instrument, because about 5 min are required for recording a spectrum, a small amount of reaction will occur during the calibration. However, the errors introduced by this means are likely to be less than the errors introduced if one performs the calibration in the absence of acid and then applies this model to the reaction which includes acid.

This paper reports the results of four types of analysis, namely two probes (MIR and UV/vis) and two types of data analysis (kinetics and PLS).

2. Theory

2.1. Experimental design for PLS calibration

In order to obtain a suitable calibration set we use systematic experimental designs. Whereas two level designs are valuable for exploratory purposes and can sometimes result in useful models, in many areas of chemistry, such as calibration, it is desirable to have several levels, especially in the case of mixture spectra [18]. A special class of design has been developed for calibration. One of the greatest problems involved [19] in the determination of multicomponent systems is the generation of a suitable training set able to predict any combination of concentrations of the compounds.

If the concentrations of two components in a training set are completely correlated, it is not possible to know whether a change in spectral characteristic results from a change in concentration of one or the other component. In addition, if a future sample arises with a high concentration for the first compound and low concentration for the second, calibration software will give an incorrect answer for the concentration of each component [19]. In mixture experiments [20,21] it is desirable that the compounds be uniformly distributed over the space. Features such as orthogonality are especially important to have a good model.

This paper employs a partial factorial design for five concentration levels ($l = 5$). Mutually orthogonal designs are only possible if the number of concentration levels is a prime number or a power of a prime number. The design requires at least l^2 experiments (25 experiments) to study a mixture [19,21]. After numbering the levels from -2 (lowest) to 2 (highest) the complete design was obtained using what is often described as a cyclic generator $(-2, 1, 2, 1, -2)$, a repeater of 0 and a difference vector $(0\ 2\ 3\ 1)$ [20]. In this type of design, there is no correlation between any concentrations of the compounds; hence, the correlation coefficient is zero.

2.2. Principal component analysis

Principal components analysis (PCA) is a technique used to discover the significant information contained in large amounts of multivariate data, and to accurately represent the data with just a few key components.

The data in this work is presented as a matrix X . Each row in the matrix represents the spectrum at one point in time. Each column represents the absorbance at a given wavelength.

The data matrix X (dimensions $I \times J$) can be decomposed [22] into a product of two matrices, as follows:

$$X = TP + E \quad (1)$$

The T matrix contains the scores of I objects on K principal components. The P matrix is a square matrix and contains the loadings of J variables on the K principal components. E is the error matrix.

If the original data matrix is dimension $I \times J$, no more than J principal components can be calculated if $J \leq I$. PC1 represents the direction in the data, containing the largest variation. PC2 is orthogonal to PC1 and represents the direction of the largest residual variation around PC1 and so on. These will contain less and less variation and therefore less information [18]. The first scores vector and the first loadings vector are often called the eigenvectors of the first principal component. Each successive component is characterized by a pair of eigenvectors.

2.3. Partial least squares

There are four steps in the application of PLS:

1. A calibration design is built with a training set, in this paper this consisted of 25 samples at 5 different concentration levels for each component.
2. The optimum number of PLS components is selected using cross-validation.
3. The prediction capacity of this model is assessed with an additional group of samples called a test set, five in this paper.
4. The model is then applied to predict the concentration profiles during the reaction period.

A detailed description is presented below.

Partial least squares (PLS) is a major regression technique for multivariate data [18,23–25]. PLS has been applied to many fields in science with great success. One important feature of PLS is that it takes into account errors in both the concentration estimates and spectra.

In this paper PLS1 was used to perform the calculations [18]. Two sets of models are obtained as follows:

$$X = TP + E, \quad c = Tq + f \quad (2)$$

where q has analogies with a loadings vector, although is not normalized. In the first equation, the product of T and P approximates to the spectral dataset obtained through the experimental work and in the second equation product of T and q approximates the concentration estimates. The common matrix in both equations is T . PLS was performed on uncentred data in this study.

It is important to determine how many significant PLS components are necessary using cross-validation. The basis of the method [19] is that the predictive ability of a model created on part of a dataset can be tested out by how well it predicts the remainder of the data. Cross-validation was employed as a method for determining how many components characterize the data. A PLS multivariate calibration model was constructed with 25 training samples and then cross validation was used for the selection of the optimum number of components (leave one out). The prediction capacity of this set was checked with an additional group of samples that had not been used in the construction of the model.

Often the error [18] is reported as a root mean square error (RMSE):

$$E = \sqrt{\frac{\sum_{i=1}^I (c_i - \hat{c}_i)^2}{D}} \quad (3)$$

where c_i is the added analyte concentration, \hat{c}_i the predicted analyte concentration, and D corresponds to the number of degrees of freedom. In addition to this absolute value, it is possible to use a relative value expressed as:

$$E(\%) = \frac{E}{\bar{c}} \times 100 \quad (4)$$

where \bar{c} is the average concentration in the data matrix.

There are three types of error that can be estimated.

The auto-predictive error, or calibration error, is calculated on the training set, so that the E corresponds to the RMSEC.

The number of degrees of freedom equals $I - K$ where K is the number of PLS components.

The cross-validation error, RMSECV, is used when performing leave one out cross-validation, the predictions are of the samples left out, and the number of degrees of freedom equals I . This error is used for the determination of the optimum number of PLS components, and a minimum in the RMSECV is taken to correspond to this optimum.

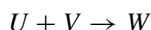
The test set or prediction error, RMSEP is calculated on an independent test set and is used to determine the quality of performance of the model. An independent test set of five samples (as described below) was used to determine this error.

Once the PLS model has been applied to the training set and validated using the test set, and demonstrated to have good predictive abilities, it can be applied to datasets where the concentration profiles are unknown, such as reaction data as described in this paper.

2.4. Kinetic modelling

In previous papers we have reported the reaction between benzophenone and phenylhydrazine [10,11] and modeled this as a second-order reaction, as expected from its chemistry. Although the rate of reaction will also be influenced by acid concentration, providing the acid is significantly in excess (as is the case in this study), the kinetics will approximate to second order. Although it is possible to compare different rate equations [26–28] whereas more complex models may fit the data better, they do not necessarily describe the reaction more accurately. In many practical cases empirical models are adequate, especially in areas such as industrial process monitoring.

Considering a second-order reaction, of the following type:



It is assumed that no side reactions take place, that there are no intermediates and that there are no impurities. The model reaction in this paper has been carefully chosen to approximate to these properties as the spectroscopy exhibits isobestic points throughout.

With these assumptions, it is possible to define this system using Eq. (5):

$$-\frac{dU}{dt} = k[U][V] \quad (5)$$

Integrating this equation, we can obtain three equations that relate to the evolution of each one of the components present in the mixture. Eqs. (6)–(8) are obtained, where Δ_0 equals $[V]_0 - [U]_0$ [27,28], and V is in excess:

$$[U]_t = \frac{\Delta_0[U]_0}{[V]_0 \exp(k\Delta_0 t) - [U]_0} \quad (6)$$

$$[V]_t = [V]_0 - ([U]_0 - [U]_t) \quad (7)$$

$$[W]_t = [W]_0 + ([U]_0 - [U]_t) \quad (8)$$

If the initial concentrations are known, using an initial guess for the value of k , it is possible to compute the concentration profiles for the compounds present in the reaction mixture. The initial guess should come from previous knowledge of the reaction being studied or, in the case no information is available a guess can be used. In this paper, the initial guess of k used assumed the reaction had reached 95% completion during the time it had been monitored. This value is obtained from previous knowledge that the reaction during the time it was monitored had nearly reached completion. For the dataset in study, the optimisation is quite robust and even when considerable error is introduced to the initial guess of the rate constant the same solution is obtained.

Once the initial guess of the concentration profiles has been established, it is necessary to optimize these profiles based on the information contained in the dataset collected during the reaction (matrix X). To this purpose, a non-linear least squares fitting was used. This method consists of several steps to complete the iterations and reach a solution. A least squares step projects the spectra X into the space spanned by C (concentration profiles) to give a matrix of the residuals, R , as shown in Eq. (9) [29]:

$$R = X - (C' C)^{-1} C' X \quad (9)$$

The non-linear least-squares procedure [30] is used to adjust the rate constants k and minimize the sum of squares residuals, $\sum r_{ij}^2$. These iterations are repeated until a solution is found that is within the limits of convergence that are defined beforehand, before starting the optimization procedure. In this case the Levenberg–Marquardt method was used for the optimization [31,32]. The algorithm can be thought of as a trust-region modification of the Gauss–Newton algorithm. It finds the minimum of a function $F(x)$ that is a sum of squares of non linear functions, as it can be seen in Eq. (10):

$$F(x) = \frac{1}{2} \sum_{i=1}^m [f_i(x)]^2 \quad (10)$$

Let the Jacobian of $f_i(x)$ be denoted $J_i(x)$, then the Levenberg–Marquardt method searches in the directions given by the solution to the equation

$$(J_k^T J + \lambda_k I) p_k = -J_k^T f_k \quad (11)$$

where λ_k are nonnegative scalars. One of the properties of the method is that, for some scalar δ related to λ_k , the vector p_k is the solution of the constrained sub problem of minimizing $\|J_k p + f_k\|_2^2/2$ subject to $\|p\|_2 \leq \delta$ [32].

In the present case, a single solution to the problem is possible, because there is a single global minimum. The convergence process is dependant on the initial guess of the rate constant.

2.5. Comparison of profiles

With the methods described in the previous section, concentration profiles are obtained for all the components present in the reaction mixture. Since we are comparing two spectroscopic techniques and two modelling techniques, we obtain four estimated profiles for each component.

Since the data is obtained from two different probes, which do not necessarily acquire spectra at in the same point in time, one has to interpolate the data acquired at a faster rate to match the one acquired at a lower rate. To this purpose, the time vector obtained from the MIR probe was used. That same vector was also used to obtain discrete points with the kinetic models that were then used in the comparison.

In order to assess the similarity of the reconstructed kinetic profiles the following equation was used:

$$\text{RMSE} = \sqrt{\frac{\sum_{i=1}^I (c_{1i} - c_{2i})^2}{I}} \quad (12)$$

where c_1 and c_2 correspond to the two profiles that are being compared.

3. Experimental

The reaction between benzophenone and phenylhydrazine to give benzophenone phenylhydrazone was monitored, using two spectroscopic probes in the reaction vessel to collect spectroscopic data simultaneously. PLS calibration was performed on 25 three-component mixtures of these compounds under conditions similar to those in the reaction vessel. Section 3.2 describes how the calibration dataset was constructed and Section 3.3 the reaction conditions.

3.1. Instrumentation

The data collection was done using a mid-infrared probe and an UV/vis probe. The SpectraProbe Linx 5-10ATR (SpectraProbe, Middlesex, UK) is a liquid phase MIR spectrometer that is capable of recording over the 1000–2000 cm^{-1} range. The spectral resolution of the detector varies between 4 cm^{-1} at 1021 cm^{-1} and 16 cm^{-1} at 1923 cm^{-1} . The attenuated total reflectance (ATR) technique is used to determine the liquid absorbances. It contains a double bounce ATR crystal and is based around a 128 element pyro-electric array. The compounds studied absorb mainly in the 1651–1196 cm^{-1} region, so only this range was used, resulting in 56 spectral data points.

For the UV/vis probe, an ATR spectroscopic probe (Hellma, Müllheim, Germany) connected by fibre optic cables to an MCS500 UV/vis spectrometer (Zeiss, Jena, Germany) was used to record all spectra. The UV/vis probe was able to record a spectrum in the range of 200–650 nm. None of the compounds studied absorbed above 400 nm, and there were strong solvent absorptions at around

Table 1
Levels and concentration data for the three compounds in the calibration set

No.	Phenylhydrazine		Benzophenone		Benzophenone phenylhydrazone	
	Level	Conc.	Level	Conc.	Level	Conc.
1	0	0.484	0	0.199	0	0.150
2	-2	0.161	-2	0.000	0	0.150
3	2	0.807	-2	0.000	-2	0.000
4	-1	0.323	2	0.397	-2	0.000
5	2	0.807	-1	0.099	2	0.299
6	0	0.484	2	0.397	-1	0.075
7	-1	0.323	0	0.199	2	0.299
8	-1	0.323	-1	0.099	0	0.150
9	1	0.645	-1	0.099	-1	0.075
10	2	0.807	1	0.298	-1	0.075
11	1	0.645	2	0.397	1	0.224
12	0	0.484	1	0.298	2	0.299
13	2	0.807	0	0.199	1	0.224
14	2	0.807	2	0.397	0	0.150
15	-2	0.161	2	0.397	2	0.299
16	1	0.645	-2	0.000	2	0.299
17	-2	0.161	1	0.298	-2	0.000
18	0	0.484	-2	0.000	1	0.224
19	1	0.645	0	0.199	-2	0.000
20	1	0.645	1	0.298	0	0.150
21	-1	0.323	1	0.298	1	0.224
22	-2	0.161	-1	0.099	1	0.224
23	-1	0.323	-2	0.000	-1	0.075
24	0	0.484	-1	0.099	-2	0.000
25	-2	0.161	0	0.199	-1	0.075

Conc.: molar concentration after adding the acid (2.878 M). Note that all calibration was performed after acid was added.

200 nm, so the spectra were only recorded in the range 220–400 nm inclusive at a 1 nm resolution, resulting in 181 data points. The path length of the UV/vis light in the probe is $\sim 3 \mu\text{m}$; hence it can be used in solutions of usual reaction concentrations.

3.2. PLS calibration and test mixture design

To obtain the calibration for both probes it was necessary to have a sample of pure benzophenone phenylhydrazone. This was achieved by performing the reaction in acetonitrile (Fisher Scientific, Laboratory Reagent Grade, UK) and letting it continue after crystallization. A recrystallization process was used to get the pure product. Purity was assessed by HPLC and the product found to be more than 99% pure.

The experimental design used is illustrated in Table 1. The different levels and concentrations in each sample for the three compounds are presented in the table. Three standard solutions of benzophenone (1.985 M), phenylhydrazine (3.581 M) and benzophenone phenylhydrazone (1.097 M) were prepared by weighing out 18.270, 19.953 and 14.942 g of the three compounds respectively and dissolving each in 50 mL of THF. From these, varying amounts were removed in different proportions to a series of 10 mL volumetric flasks to produce 25 mixtures with THF as the solvent. A 5 mL was removed from each of the flasks and 1 mL glacial acetic acid added to produce a sample for spectroscopic measurement. The solution was shaken and immediately analyzed by both

probes. It is important to have these samples prepared only a few s prior to recording the spectra since the addition of acid catalyses the reaction.

The concentration after adding the acid (2.878 M) is shown in Table 1. Cross validation was used to select the number of PLS components for each of the components. A test-set with five samples was used to investigate the performance of the models created. Table 2 shows the molar concentration used for these five samples.

3.3. Reaction

The reaction studied involved the addition of phenylhydrazine to benzophenone to give benzophenone phenylhydrazone (see Fig. 1).

The reaction is suitable for monitoring via UV/vis and MIR spectroscopy [10,11]. The reactants and the product have prominent regions where they absorb in both of the

Table 2
Concentration data for the three compounds in the test set

No.	Phenylhydrazine (conc.)	Benzophenone (conc.)	Benzophenone phenylhydrazone (conc.)
1	0.645	0.397	0.150
2	0.484	0.298	0.224
3	0.161	0.199	0.299
4	0.807	0.000	0.075
5	0.323	0.099	0.000

Conc.: molar concentration after adding the acid (2.878 M).

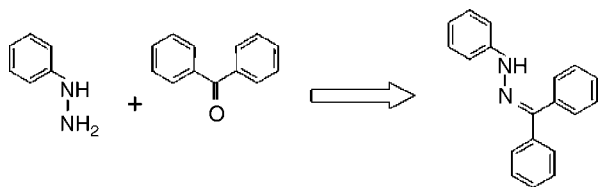


Fig. 1. Reaction scheme between phenylhydrazine and benzophenone to give benzophenone phenylhydrazone.

spectroscopic techniques used. Therefore, it is possible to study the change in composition of reaction mixture by monitoring the reaction with both probes. The data acquired can be seen in Fig. 2. The reaction occurs at a reasonable rate and the data can be acquired relatively quickly. The pure normalized UV/vis and MIR spectrum of a sample of each compound is shown in Fig. 3. As one can see the spectra

of the compounds overlap in most of the regions of greatest absorbance. An important step will be to deconvolute the signal obtained in this work.

The reaction was carried out using a molar ratio of 2.03:1 phenylhydrazine to benzophenone. 4.448 g (1.596 M) of phenylhydrazine (Lancaster, 97%, UK) were accurately weighed and transferred to a 25 mL volumetric flask and made up with tetrahydrofuran (THF) (Fisher Scientific, Laboratory Reagent Grade, UK). 3.686 g (0.801 M) of benzophenone (Fluka, 99%, Switzerland) were accurately weighed and the same procedure as above was performed.

A three-necked round-bottomed flask was set up with the necks of the flask fitted with a MIR probe, UV/vis probe and overhead stirrer. An oil bath was used to control the temperature, since the temperature is a very important factor in all kinetic studies. The bath was heated to 25 °C. A 20 mL of

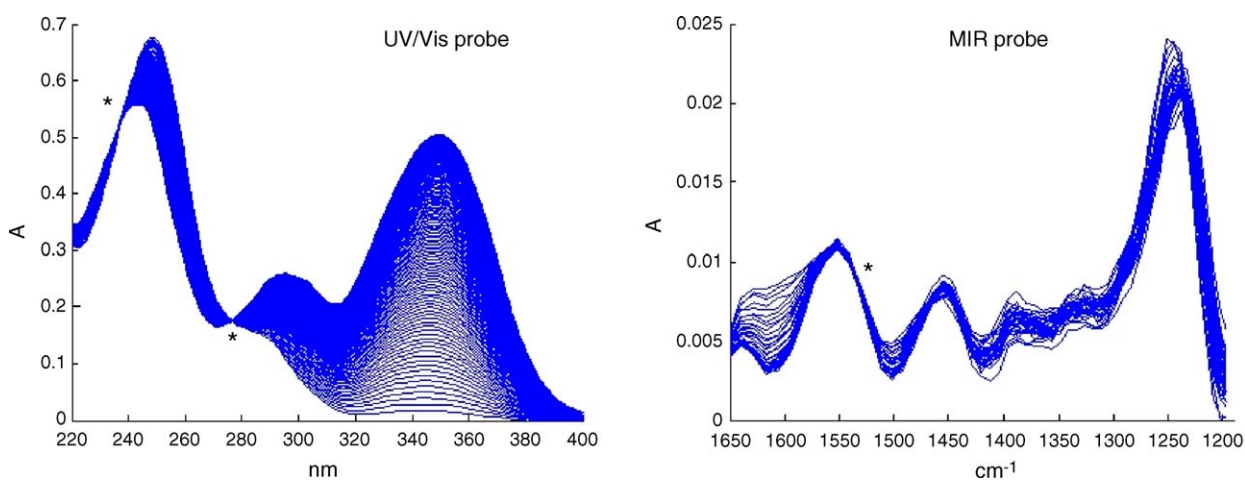


Fig. 2. Reaction spectra taken over time of the reaction with both probes. The mark (*) shows the isosbestic points.

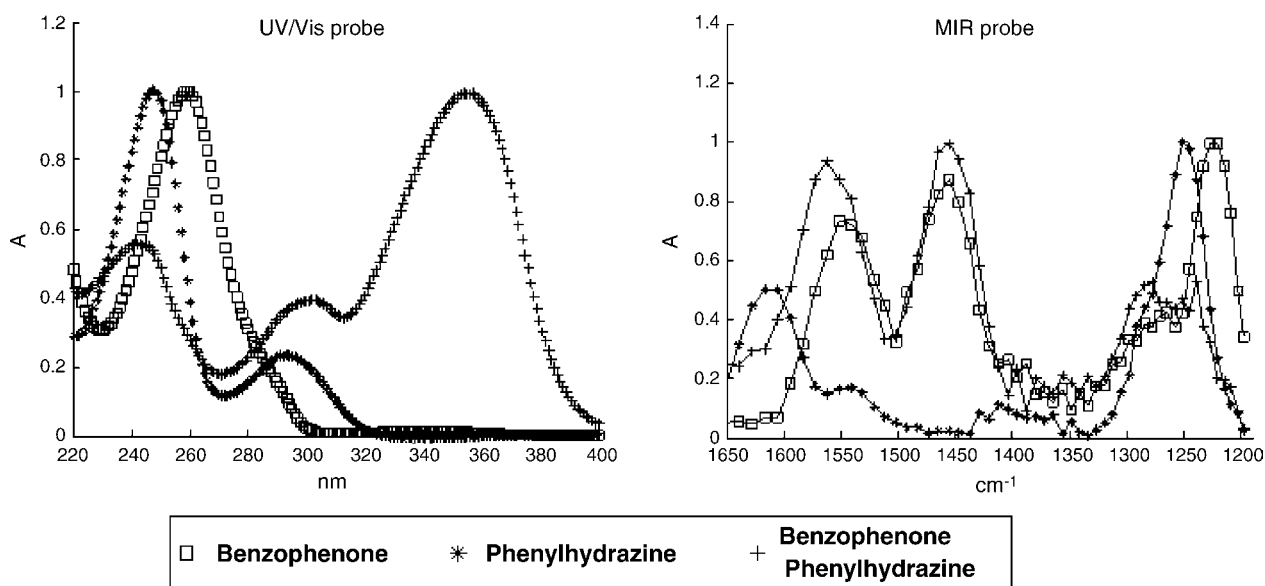


Fig. 3. Normalized pure spectra of the three reaction compounds.

each of the two solutions were transferred into the round bottomed flask and left to equilibrate. The mixture of reactants was monitored by both probes, and it was confirmed that no reaction occurred. When the mixture reached the required reaction temperature, 8 mL of glacial acetic acid (Fisher Scientific, Laboratory Reagent Grade, UK) was added. The acid (2.878 M) works as the catalyst of the reaction, hence the reaction only starts once the acid is added. Since there is no reaction before this point, there are no changes in the spectra so monitoring is only useful after the addition of acid. There was a 15 s delay between when the acid was added until the first spectrum was recorded to allow mixing of the components present in the mixture. Spectra were recorded every 60 s for UV/vis probe and every 5 min for MIR probe. In the case of the MIR probe the longer time reflects the need to obtain adequate signal to noise ratio. The UV/vis probe collected 125 spectra, and last was measured 7455 s after adding the acid. The MIR probe collected 36 spectra, with data recorded until 10 955 s. The longer acquisition time reflects the need to have enough information to use the methods presented in Section 2. The MIR data set matrix contains 36 measurements of the reaction at different times (rows) and

56 variables (columns). The UV/vis data matrix has dimensions 125×181 .

4. Results and discussion

4.1. Reaction spectra

The reaction was run and monitored at the same time by both probes according to Section 3. For UV/vis spectra, changes of spectra can be understood by dividing the wavelength in three groups. The absorption increases for the first 18 variables (220–237 nm), then it decreases until 277 nm and finally it increases again until 400 nm. These regions are defined by two points where there is no change in absorption throughout the duration of the reaction (isosbestic points) and they are a good indication of a reaction with no side products (Fig. 2). These points will be lost if a change in reaction conditions occur, for example crystallization of the benzophenone phenylhydrazone or changes in the temperature as the reaction progresses or presence of an intermediate. Spectra obtained

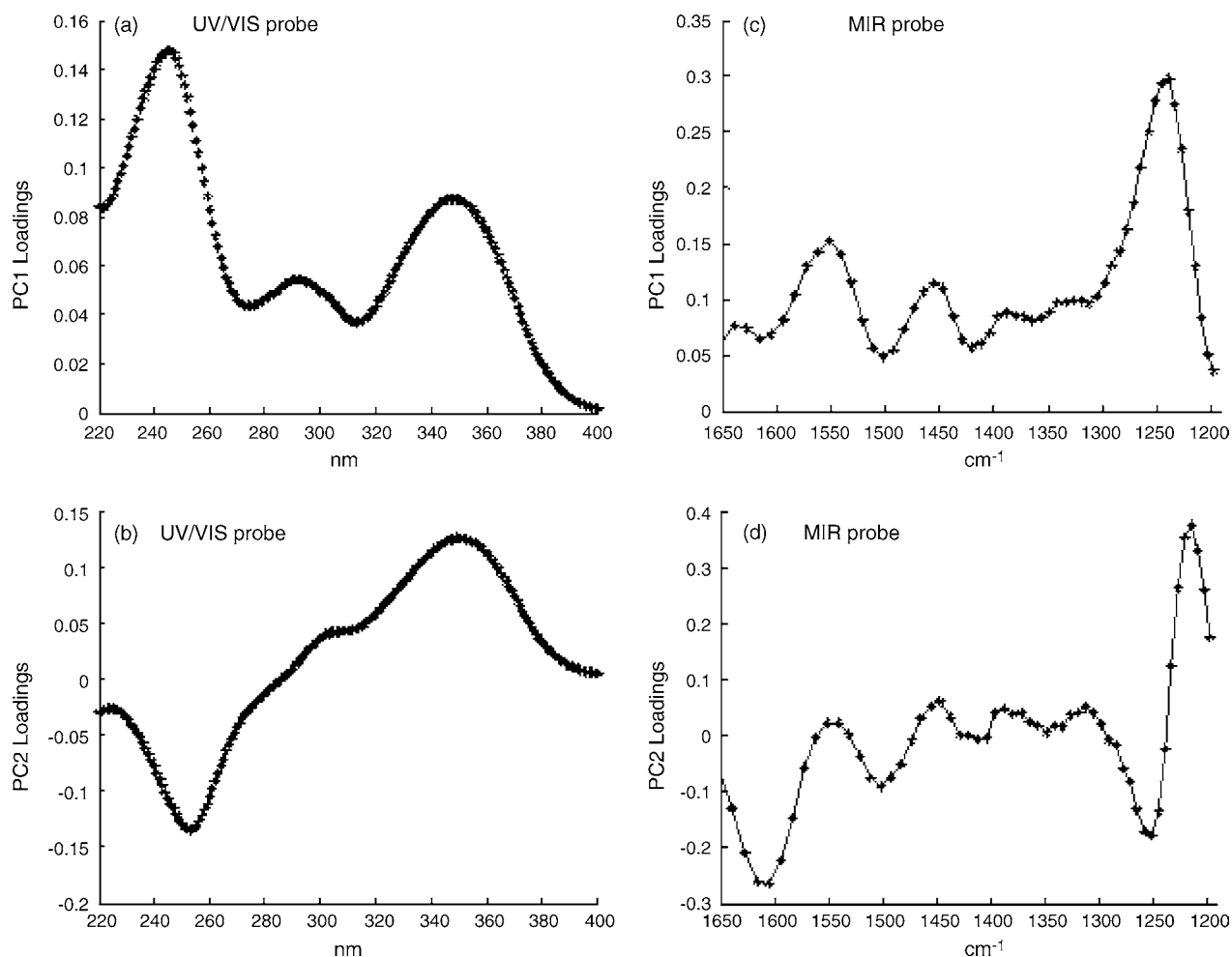


Fig. 4. PCA loadings on the raw data from the reaction obtained with UV/vis probe (a and b) and MIR probe (c and d).

from the MIR probe also show the presence of an isosbestic point.

4.2. Principal component analysis

The use of PCA gives an approximate idea of what is occurring when the reaction is progressing. PCA was performed on the raw data obtained from the reaction measured by both probes. The principal results are shown in Figs. 4 and 5. The first PC relates to the total intensity of the spectra. The loading plots for UV/vis and MIR data represent a combination of three pure spectra for benzophenone phenylhydrazone, benzophenone and phenylhydrazine. Fig. 4a and c shows these combinations. One can see that they agree well with the individual spectra for three compounds (Fig. 3) in terms of shape. However, there are some differences between the overall intensity for each variable and the loadings plot for the same variable because the individual spectra are normalized while the PC1 loadings graphs were obtained with all data taken from the reaction. The second PC relates primarily to the change in shape of the spectra during the reaction. The loadings plots (Fig. 4b and d) show how each variable

changes relative to the others over the course of the reaction, with the variables with the largest negative values corresponding to those whose intensity decrease the most during the course of the reaction. Correspondingly, the variables with the largest positive values relate to those ones that increase the most. The first variables are related to reagents and the last ones represent the product. In the case of the MIR data, the two wavenumbers with the largest negatives values are 1605 and 1251 cm^{-1} and are representative of the reagents, mainly benzophenone. The variable with the highest positive value (1214 cm^{-1}) accounts primarily for the product. In the scores plot shown in Fig. 5, one can see an increase evolution from negative to positive with time. The second PC score increases until the reaction finishes and is a good indication of the reaction profile.

All the qualitative results obtained from the probes, when PCA is performed, show the development of the reaction during the course of time, being a first indication of the behaviour of the compounds.

4.3. PLS models of calibration and test set

In order to obtain concentrations profiles for both reagents and the product during the reaction period it is necessary to develop an appropriate calibration set. To this purpose, a partial factorial design at five levels was employed.

Using the 25 samples of the calibration set, PLS models were obtained for each compound. For the cross-validation the *c* block was used. The significant minimum root mean standard error of validation value for cross-validation (leave one out) occurred for benzophenone phenylhydrazone, benzophenone and phenylhydrazine at 7, 6 and 7 PLS components for MIR data and 5, 5 and 5 PLS components for UV/vis data respectively. The number of components was chosen by graphical investigation of the plot of the RMSECV versus the number of components. These plots are illustrated in Fig. 6. The relatively high number of PLS components for both MIR and UV/vis data can be explained if one takes into account the pure spectral similarity of the three compounds studied.

The calibration worked satisfactorily and the prediction results for the “test set” which had not been used in the construction of the model are shown in Table 3. The RMSEP

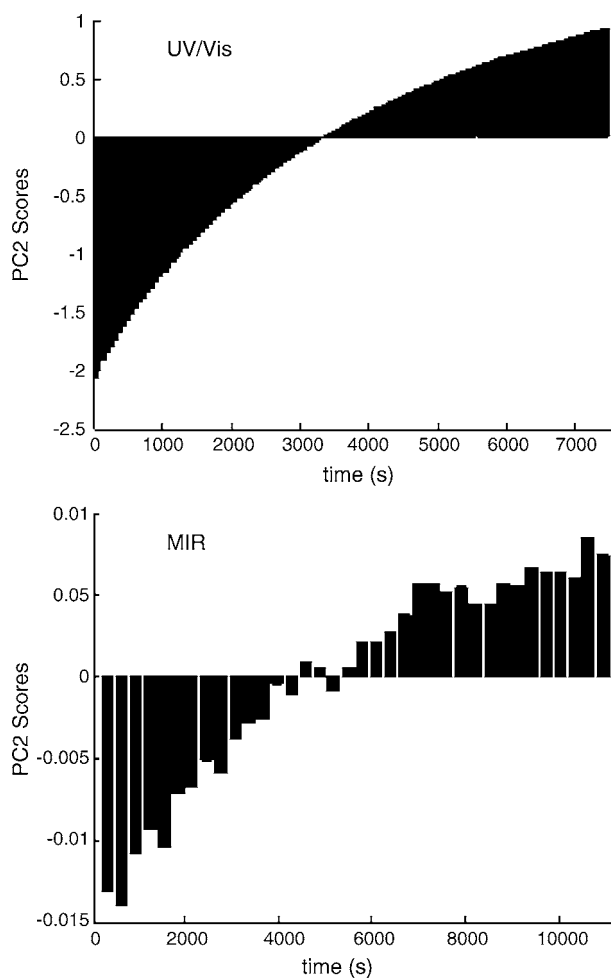


Fig. 5. PCA scores on the raw data from the reaction obtained with both probes.

Table 3
Prediction results of test set

Compound	Probe	Test set	
		<i>E</i> (M)	<i>E</i> _%
Phenylhydrazine	MIR	0.0113	2.3
	UV/vis	0.0214	4.3
Benzophenone	MIR	0.0062	3.0
	UV/vis	0.0101	5.0
Benzophenone phenylhydrazone	MIR	0.0082	5.3
	UV/vis	0.0093	6.0

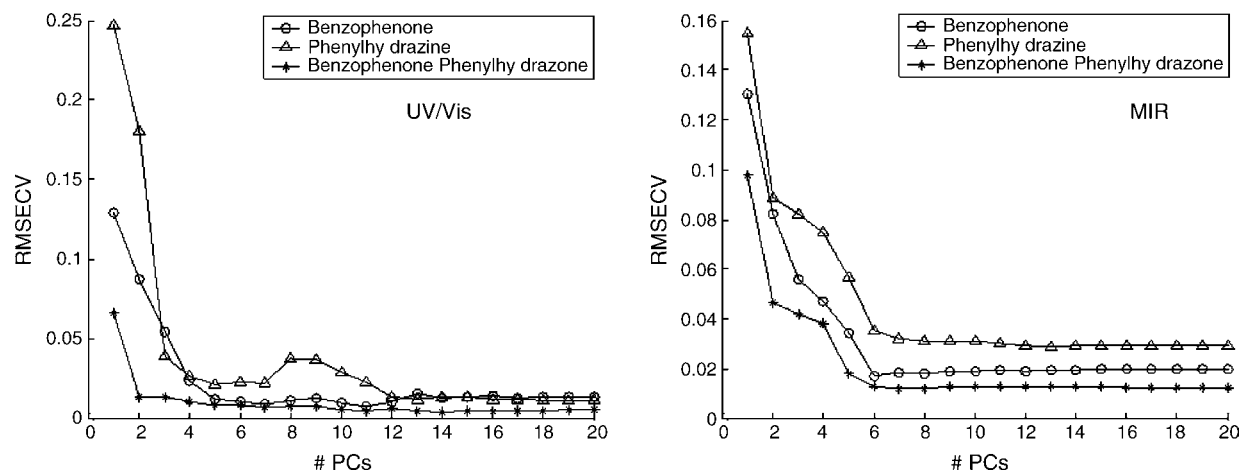


Fig. 6. Plots of the RMSECV vs. # PCs for both datasets.

values ranged between 0.0062 and 0.0214 mol/L. The predictions errors are similar in magnitude for both probes, even though each MIR spectrum was acquired during 5 min to increase the signal to noise ratio and improve the result. In the case of the UV, spectra are acquired over a period of ms.

4.4. Kinetic modelling

With the datasets collected during the run of the reaction, using the initial concentrations and the method shown above, it is possible to model the concentration profiles of the compounds present in the reaction mixture. Since we are forcing the concentration profiles to obey a second-order profile, this method is sometimes also called hard modelling.

The weighed initial concentrations of the reactants are used as the initial concentration of the compounds, so there is perfect agreement between the actual measured initial concentrations and the ones shown with the hard model.

For the MIR probe we obtain the concentration profiles seen in Fig. 7. The value of the rate constant k obtained was $4.02 \times 10^{-4} \text{ M}^{-1} \text{ s}^{-1}$. Only spectra acquired after adding the

acid to reaction were used since that is when the reaction actually started. One can observe that the reaction still had not reached completion, although it was close.

Using the same procedure with the UV/vis probe the profiles shown also in Fig. 7 were obtained. The value obtained for the rate constant was $4.34 \times 10^{-4} \text{ M}^{-1} \text{ s}^{-1}$. The value for the rate constant is quite similar to the one obtained in the case of the MIR probe, which means that similar concentration profiles and comparable information was extracted from different datasets.

Comparing the profiles from the MIR and UV/vis probes one can see that they are quite similar. This is a consequence of the similarity in the rate constants obtained.

4.5. Comparison between PLS and kinetic models

Although soft modelling and hard modelling in essence rest on quite different properties, their aim is similar and they should, produce the same numerical results, providing the assumptions are similar [20].

The data was investigated using both techniques, for both the UV/vis probe and for the MIR probe. This means that four concentration profiles were obtained for each compound present in the reaction mixture. The two profiles from the kinetic models and two profiles from PLS models obtained from both probes can be obtained as illustrated in Fig. 7. Note that the profiles from hard modelling involve estimating a rate constant and then producing a profile using this estimate and the initial concentrations. For soft modelling the concentrations are calculated at each point in time using PLS.

Observing Fig. 7, one can see that the concentration profiles for the compounds are quite similar using both data analytical techniques and both probes. The quality of agreement between the methods can be assessed numerically using approaches of Section 2.5, see Table 4. The highest error is observed when comparing the PLS profiles for phenylhydrazone. The reason is the big difference in the estimation of the initial points in time using PLS. This is expected since it

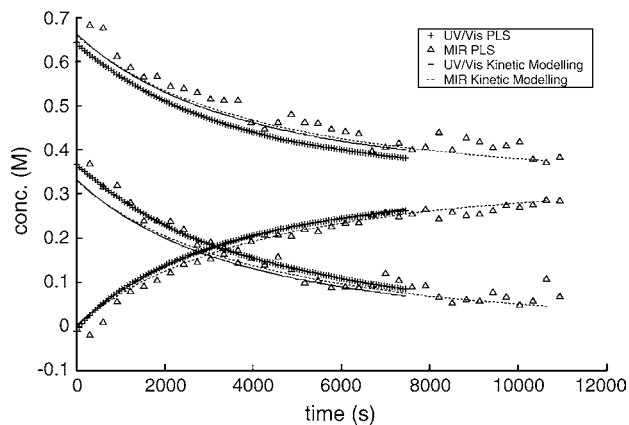


Fig. 7. Concentration profiles obtained with soft modelling (PLS) and hard modelling (HM) for both UV/vis and MIR probe.

Table 4
Comparison of the errors computed between the concentration profiles obtained for both modelling and spectroscopic techniques

RMSE (M)	UV/vis PLS model	MIR PLS model	UV/vis kinetic model	MIR kinetic model
(a) Phenylhydrazine				
UV/vis PLS model	0			
MIR PLS model	0.046	0		
UV/vis kinetic model	0.020	0.028	0	
MIR kinetic model	0.027	0.023	0.007	0
(b) Benzophenone				
UV/vis PLS model	0			
MIR PLS model	0.016	0		
UV/vis kinetic model	0.026	0.031	0	
MIR kinetic model	0.020	0.027	0.007	0
(c) Benzophenone phenylhydrazone				
UV/vis PLS model	0			
MIR PLS model	0.022	0		
UV/vis kinetic model	0.003	0.021	0	
MIR kinetic model	0.009	0.016	0.007	0

See Eq. (12) for details.

is common in PLS modelling that the first points have a high error due to mixing and dissolution problems. This problem also affects the comparison of PLS with kinetic results. In kinetic modelling the initial concentrations are calculated from weighing, and therefore in some of the profiles there is a significant difference in the first points to those from PLS. Since hard models consider the data as a whole, they are not so susceptible to this type of error. The lowest errors are obtained when comparing kinetic profiles. This is due to the fact that kinetic profiles do not contain oscillations in the predicted concentrations, since they obey kinetic equations.

Fitting second-order kinetic equations to the PLS model, we can obtain estimates of the rate constant and have a numerical comparison. For the PLS model of the UV/vis data, a value of $4.29 \times 10^{-4} \text{ M}^{-1} \text{ s}^{-1}$ was obtained for k . For MIR, the fitted k is $3.51 \times 10^{-4} \text{ M}^{-1} \text{ s}^{-1}$. This demonstrates that one can monitor this particular reaction using both UV/vis techniques and MIR techniques and hard and soft modelling. It also gives confidence in the estimations made since in one we assumed that we were using a second-order reaction and in the other one, no assumption was made.

The results are also consistent with the assumptions about the mechanism of the reaction, both that there is second-order kinetics and that there are no significant side reactions or intermediates, otherwise the profiles obtained with both modelling methods would probably be different. If one is not sure about the reaction mechanism, PLS models are recommended.

5. Conclusion

On-line reaction monitoring is a fast developing area in chemometrics, with increasing number of techniques, methods and equipment. Miniaturization of spectroscopic equipment allows to acquire a larger amount of data and to analyze this data immediately.

Monitoring a reaction with several probes allows to obtain increasingly diverse data and to acquire supplementary reaction information. In this paper, it was proven that it is possible to use different techniques and chemometrics methods and achieve similar quality of information, allowing us to confirm the results obtained.

In this paper both PLS and kinetics models were used to analyze the data. The assumptions made in the hard models were proven, with not only the graphical visualization of the spectra taken during the reaction but also with the agreement between both types of models. It is shown that concentration profiles can be obtained using both UV/vis data and MIR data, with the same level of accuracy, even if the acquisition time differs due to instrumental restrictions.

Chemometrics is a useful tool for monitoring reactions, obtaining concentration profiles and estimation of reaction end-points (e.g. at what time a reaction will reach 99% completion) and product maxima (especially if the product is an intermediate in a multistage reaction). Whereas the acceptance of such techniques in on-line reaction monitoring is developing gradually, new technologies, such as using more than one probe, pose new challenges to the analytical chemist who wishes to employ chemometric techniques.

Acknowledgements

We thank David Baines and Ian Weaver from Spectraprobe for loan of the Spectraprobe Linx 5-10ATR spectrometer. A.R.C. acknowledges GlaxoSmithKline and the University of Bristol for financial support. M.N.S. acknowledges the DGICYT (Project BQU2001-1858), the Consejería de Educación y Cultura of the Junta de Castilla y León and the Unión Europea (Fondo Social Europeo, Project SA079/02) for financial support and also the grant awarded by the Junta de Castilla y León.

References

- [1] T. Rohe, W. Becker, S. Kölle, N. Eisenreich, P. Eyerer, *Talanta* 50 (1999) 283.
- [2] C. Coffey Jr., B.E. Cooley, D.S. Walker, *Anal. Chim. Acta* 395 (1999) 335.
- [3] N. Kettaneh-Wold, *Chemom. Intell. Lab. Syst.* 14 (1992) 57.
- [4] H.J. Luinge, J.H. van der Maas, T. Visser, *Chemom. Intell. Lab. Syst.* 28 (1995) 129.
- [5] A.C. Quinn, P.J. Gemperline, B. Baker, M. Zhu, D.S. Walker, *Chemom. Intell. Lab. Syst.* 45 (1999) 199.
- [6] O. Svensson, M. Josefson, F.W. Langkilde, *Chemom. Intell. Lab. Syst.* 49 (1999) 49.
- [7] T.J. Thurston, R.G. Brereton, *Analyst* 127 (2002) 659.
- [8] R. Tauler, R. Gargallo, M. Vives, A. Izquierdo-Ridorsa, *Chemom. Intell. Lab. Syst.* 46 (1999) 275.
- [9] A.R. Carvalho, R.G. Brereton, T.J. Thurston, R.E.A. Escott, *Chemom. Intell. Lab. Syst.* 71 (2004) 47.
- [10] T.J. Thurston, R.G. Brereton, D.J. Foord, R.E.A. Escott, *J. Chemomet.* 17 (2003) 313.
- [11] T.J. Thurston, R.G. Brereton, D.J. Foord, R.E.A. Escott, *Talanta* 63 (2004) 757.
- [12] M.L. Kieke, J.W. Schoppeldrei, T.B. Drill, *J. Phys. Chem.* 100 (1996) 7455.
- [13] W.S. Rayens, A.H. Andersen, *Chemom. Intell. Lab. Syst.* 71 (2004) 121.
- [14] S. Wold, N. Kettaneh, H. Fridén, A. Holmberg, *Chemom. Intell. Lab. Syst.* 44 (1998) 331.
- [15] J. Helminen, M. Leppämäki, E. Paatero, P. Minkkinen, *Chemom. Intell. Lab. Syst.* 44 (1998) 341.
- [16] H. Haario, K. Steen, H. Martens, *Chemom. Intell. Lab. Syst.* 44 (1998) 77.
- [17] V.M. Taavitsainen, H. Haario, *J. Chemomet.* 15 (2001) 215.
- [18] R.G. Brereton, *Chemometrics Data Analysis for the Laboratory and Chemical Plant*, Wiley, Chichester, 2003.
- [19] R.G. Brereton, *Analyst* 125 (2000) 2125.
- [20] R.G. Brereton, *Analyst* 122 (1997) 1521.
- [21] J. Aybar Muñoz, R.G. Brereton, *Chemom. Intell. Lab. Syst.* 43 (1998) 89.
- [22] D.L. Massart, B.G.M. Vandeginste, L.M.C. Buydens, S. de Jong, P.J. Lewi, J. Smeyers-Verbeke, *Handbook of Chemometrics and Quality Metrics: Part A*, Elsevier, Amsterdam, 1997, p. 535.
- [23] M.F. Delaney, *Chemom. Intell. Lab. Syst.* 3 (1988) 45.
- [24] H. Martens, T. Naes, *Multivariate Calibration*, Wiley, Chichester, 1989, p. 116.
- [25] P. Geladi, B.R. Kowalski, *Anal. Chim. Acta* 185 (1986) 1.
- [26] Z.L. Zhu, W.Z. Cheng, Y. Zhao, *Chemom. Intell. Lab. Syst.* 64 (2002) 157.
- [27] J.H. Espenson, *Chemical Kinetics and Reaction Mechanisms*, 2nd ed., McGraw-Hill, New York, 1995, p. 90.
- [28] E. Bezemer, S.C. Rutan, *Chemom. Intell. Lab. Syst.* 59 (2001) 19.
- [29] NIST Sematech e-Handbook of Statistical Methods, 2004. <http://www.itl.nist.gov/div898/handbook/>.
- [30] K. Levenberg, *Quart. Appl. Math.* 2 (1944) 164.
- [31] D. Marquardt, *SIAM J. Appl. Math.* 11 (1963) 431.
- [32] P.R. Gill, W. Murray, M.H. Wright, *The Levenberg–Marquardt Method*, Academic Press, London, 1981, p. 136.